Photoinitiator-free Two-photon Polymerization of Biocompatible Materials for 3D micro/nano Fabrication

*Atsushi Nakayama, Yasuaki Kumamoto, Masafumi Minoshima, Kazuya Kikuchi, Atsushi Taguchi, and Katsumasa Fujita**

A. Nakayama, Y. Kumamoto, K. Fujita

Department of Applied Physics, Osaka University, Suita, Osaka 565-0871, Japan

E-mail: fujita@ap.eng.osaka-u.ac.jp

A. Nakayama, K. Fujita

AIST-Osaka University Advanced Photonics and Biosensing Open Innovation Laboratory, National Institute of Advanced Industrial Science and Technology (AIST), Suita, Osaka 565-0871, Japan

M. Minoshima, K. Kikuchi

Division of Applied Chemistry, Osaka University, Suita 565-0871, Japan

K. Kikuchi

Immunology Frontier Research Center, Osaka University, Suita 565-0871, Japan

A. Taguchi

Research Institute for Electronic Science, Hokkaido University, Sapporo, Hokkaido 001-0020, Japan

K. Fujita

Transdimensional Life Imaging Division, Institute for Open and Transdisciplinary Research Initiatives, Osaka University, Suita, Osaka 565-0871, Japan

Keywords: two-photon polymerization, initiator-free, DUV absorption, hydrogel, collagen

Two-photon polymerization is expected to realize the fabrication of biological tissues for regenerative medicine and drug development because of its capability of three-dimensional fabrication with submicrometer spatial resolution. However, photopolymerization initiators generally added to resins have low biocompatibility and water solubility, which pose a challenge for the biological application of micro- and nano-structures fabricated by photopolymerization. In this study, we perform two-photon polymerization using biocompatible materials without photoinitiators and evaluated the preservation of the material properties of the fabricated 3D structures. Poly(ethylene glycol) diacrylate (PEGda) and collagen have been successfully fabricated using a femtosecond pulsed laser at a wavelength of 400 nm with a feature size of 100 nm without photoinitiator. The excitation intensities required for the polymerization of PEGda and collagen are about 450 kW/cm^2 and 150 kW/cm^2, respectively, which are smaller than those reported with using photoinitiators. Raman spectroscopy is used to confirm that the water-swelling polymer network of PEGda and the enzymatic degradation of collagen, which are important factors in the application with live cells, are maintained in the fabricated structures.

1. Introduction

Two-photon polymerization (TPP) can be used to fabricate three-dimensional micro/nanostructures with a feature size beyond the diffraction limit of light [1,2]. TPP fabrication has been used in biological applications such as cell culturing [3–5], tissue engineering[6,7], and microfluidics [8,9]. In biological applications, arbitrary 3D fabrication with a submicron feature size has the potential to reproduce 3D scaffolds with subcellular-scale structures for organ printing or with precisely controlled geometry for systematic study of cellular behavior at the single-cell level.

One of the challenges in the biological applications of TPP is the development of photoinitiators to be added to photopolymerizable resins. When a near-infrared (NIR)

femtosecond pulsed laser beam is used for the excitation of TPP, the photoinitiator absorbs two photons of NIR light and generates radicals to trigger a free-radical polymerization reaction. For bio-applications in TPP, photoinitiators must have less cytotoxicity and high solubility in an aqueous medium, as well as a large two-photon absorption cross-section to increase the efficiency of radical generation. However, photoinitiators in a resin typically reduce the survival rate of cells cultured on the microstructures made of the resin[3,10,11], which has hindered the biological applications of TPP.

Recently, TPP without the addition of photoinitiators has been conducted using visible femtosecond pulsed laser light[12,13]. Two-photon absorption using visible light can directly excite functional groups of monomers, such as C=C, C=O, or aromatic compounds, which have strong absorption in the deep UV region from 200 to 300 nm, to realize two-photon polymerization (deep-UV two-photon polymerization, DUV-TPP) of the monomers. By using a wavelength of 530 nm[12], the 3D fabrication of microstructures of proteins (bovine serum albumin and human serum albumin) has been demonstrated. Taguchi et al. reported TPP using femtosecond laser pulses with a wavelength of 400 nm and presented the 3D nano-fabrication of pure acrylate monomer/oligomer with a feature size of 80 nm[13]. Because shorter excitation wavelengths have higher photon energy and can excite a greater variety of chemical bonds related to photopolymerization, this can polymerize various materials without photoinitiators. Moreover, we found that the excitation laser power required for fabrication using 400-nm femtosecond pulses was lower than that using NIR pulses and photo-initiators because the monomers absorbing light to start polymerization are high in concentration.

In this study, we applied DUV-TPP to photoinitiator-free polymerization of bio-practical materials. We performed DUV-TPP of PEGda as a hydrogel material and collagen as a typical extracellular matrix (ECM) protein in biological tissue, which have been used in various biological applications. It is important to investigate the chemical properties of biomaterials upon DUV-TPP to understand how the materials are chemically modified at two-

photon polymerization without photoinitiators and determine the extent to which the intrinsic properties are preserved. By comparing the Raman spectra before and after irradiation with visible pulses, we examined the chemical reaction in direct two-photon excitation polymerization without photoinitiators. We confirmed that the hydrogel response to water and enzymatic degradation of collagen were preserved in the fabricated microstructures.

2. Result and Discussion

2.1. DUV-TPP of PEGda

We used PEGda with an average molar mass of 700 g/mol to demonstrate the DUV-TPP of hydrogels without a photoinitiator. PEGda is a biocompatible and low-cytotoxic hydrogel that has been used for the 3D microfabrication of hydrogel structures by NIR-TPP with photoinitiators [3,14–17]. PEGda has two C=C bonds per molecule (**Figure 1**A). It does not exhibit light absorption in the visible region but, in the DUV region (around 200 nm), as shown in Figure 1A and did not show photopolymerization under irradiation of CW laser light with a wavelength of 405 nm (Figure S1). We expected photopolymerization of PEGda with two-photon excitation using visible femtosecond pulses.

A micro-woodpile structure of PEGda was fabricated with 400-nm femtosecond pulsed excitation. Figure 1B shows the SEM image of the microwoodpile structure fabricated using pure PEGda as a material. The structure was designed with the volume of 5 μm×5 μm×5 μm and the periodicity of 0.5 μm and 0.3 μm in lateral and axial, respectively.

The 3D structure of PEGda was fabricated without photoinitiators as designed. Figure 1C shows the SEM image of the area indicated by the dotted rectangle in Figure 1B. The linewidth at the top of the 3D microstructure is 100 nm. By utilizing the effect of shrinkage during development[18,19], we achieved a linewidth of 30 nm for a suspended nanowire when we used 4arm-PEG acrylate as a monomer (Figure S2).

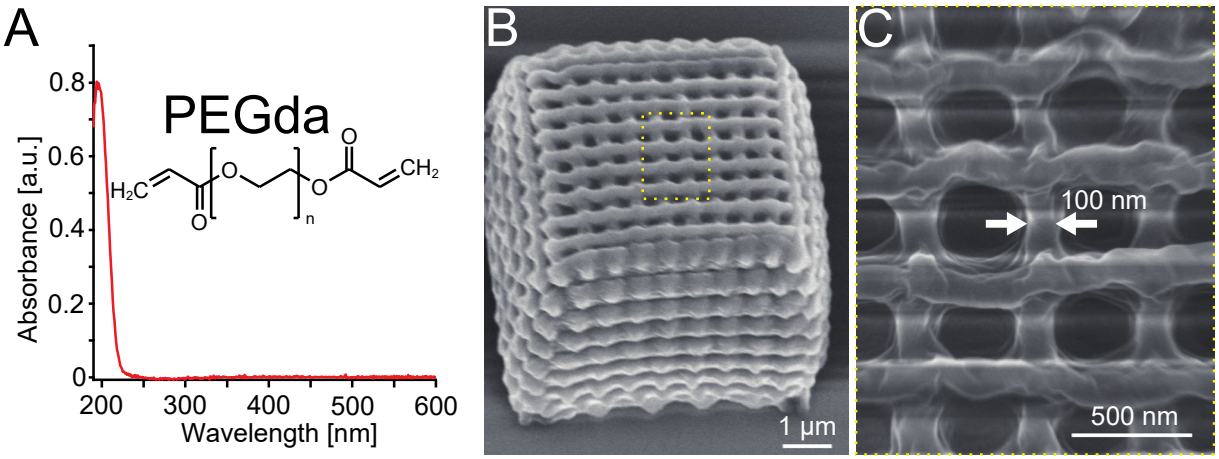

Figure 1. DUV-TPP of PEGda. (A) UV-Visible absorption spectrum of PEGda and its molecular structure. (B) SEM images of 3D microstructures with a nano-feature size. The excitation intensity was 485 kW/cm^2. (C) SEM image magnified in (B).

We fabricated a PEGda cube with a side of 5 μm by adjusting the excitation intensity from 0 kW/cm^2 to 708 kW/cm^2 to understand the effect of the excitation intensity. **Figure 2**A shows an optical bright-field image of the microcubes fabricated with excitation intensities from 99 kW/cm^2 to 708 kW/cm^2. While an excitation intensity smaller than 436 kW/cm^2 was not sufficient for DUV-TPP, an excitation intensity over 708 kW/cm^2 caused the structure to explode (Figure S3).

To understand the chemistry of DUV-TPP, we performed *in situ* Raman analysis. Figure 2B shows the Raman spectra of PEGda irradiated with a 400 nm femtosecond pulsed laser beam at various excitation intensities, together with the Raman spectrum of pure PEG. The Raman spectra of PEGda after DUV-TPP still have specific Raman peaks of PEG, indicating that the fabricated microstructures possess a chemical structure similar to that of PEG.

We plotted the Raman peak intensities to the DUV-TPP excitation intensity for several Raman bands in Figure 2C. The Raman peak intensities are normalized by the intensity of O-CH_2 deformation at 1470 cm^{-1}, with an assumption that O-CH_2 was not altered by the polymerization reaction [20] and could be used as an internal reference. Hence the difference in the detection volume in each measurement was canceled in the plot. We also normalized each

plot by the Raman peak intensity at an excitation intensity of 0 kW/cm^2, where no Raman peak was affected by DUV-TPP. Figure 2C clearly shows the threshold in the excitation intensity that alters Raman spectrum; there was no significant change in the peak intensity of any of the Raman peaks at excitation below 380 kW/cm^2, whereas above 436 kW/cm^2, the plots show decreases or increases in the Raman peak intensity. The threshold excitation intensity also corresponds to the intensity that separates successful and unsuccessful fabrication in bright-field observations shown in Figure 2A.

The decreased Raman peaks at 1411 cm^{-1}, 1636 cm^{-1}, 1722 cm^{-1}, 3113 cm^{-1}, and 3041 cm^{-1} are related to the alkene C=C and C=O bonds, similar to the responses observed in the DUV-TPP of acrylate resin[13]. The decrease in these Raman intensities indicated that the C=C bonds were consumed via their cleavage by photoexcitation. The decrease in the C=O Raman peak was presumably caused by the collapse of conjugation with the cleaved C=C bonds[21,22]. Associated with the cleavage of C=C bonds, the loss of molecular planarity occurred and the reduction in the in-plane CH_2 deformation vibration was caused. These Raman intensities decrease nonlinearly with excitation intensity, indicating that the photopolymerization of PEGda under visible femtosecond-pulse irradiation was induced by a two-photon process. The increase in Raman peaks at 2889 cm^{-1} and 2950 cm^{-1}, assigned to the symmetric or asymmetric CH_2 stretching vibration in C-C bonds, can be explained by the increase in the number of C-C bonds generated from the C=C bonds via their cleavage.

At the excitation intensities between 493 and 708 kW/cm^2, the Raman intensity increase and decrease became subtle, and Raman intensities related to C=C bonds converged to 0.2 approximately. According to literature, approximately 20% of the acrylate monomer remains unreacted during the polymerization reaction at room temperature[23,24]. In our study, the photopolymerization reaction became saturated, and unreacted monomers remained in the fabricated structure. The degree of conversion from monomer to polymer in DUV-TPP can be estimated at 80% from Raman spectroscopy. The value is equal to or higher with

photoinitiators in one-photon[25] and two-photon polymerization[26,27]. Because the higher conversion rate exhibits larger mechanical strength of photo-induced polymer[27,28], our result suggests no significant difference in mechanical properties between with and without photoinitiators in two-photon polymerization. Also, this result indicates that cytotoxicity effect from unreacted monomer in a microstructure using DUV-TPP is not larger than that using a photoinitiator in one-photon and two-photon polymerization.

We also polymerized 4arm-PEG acrylate with DUV-TPP and performed *in situ* Raman analysis of the fabricated structures. With the Raman analysis, we confirmed that the intensity decrease in Raman peaks was attributed to C=C bonds and the intensity increase in Raman peaks was attributed to C-C bonds. (Figure S4). The changes in the Raman peaks occurred with a lower excitation intensity (21 kW/cm^2) than that for the case of PEGda. This is because the greater number of functional groups exists in the C=C bonds per molecule.

The lowest excitation intensity of 436 kW/cm^2 for DUV-TPP of PEGda is less than one-fourth of the energy required in the previous report where 535-nm femtosecond pulses were focused by an NA-1.4 objective lens for two-photon excitation of PEGda (700 Mn) with a photo-initiator (HMPP)[29]. About half of the recent publications used an NA-1.4 and the exposure time similar to our experiments [17,30]. The smaller excitation threshold with photoinitiators was due to the higher concentration of excited species. The resin consisting of 100% PEGda was directly excited in DUV-TPP. On the other hand, in the case of using photoinitiators in NIR-wavelength excitation, the concentration of the photoinitiator is typically less than 1 wt% in the resin to avoid cytotoxicity. We experimentally compared the excitation threshold of TPP using a photoinitiator of Irgacure 369 and NIR-wavelength excitation (Figure S5). The result shows that DUV-TPP has an excitation threshold smaller than TPP by NIR light using photoinitiators with a concentration less than 2.0 wt%. This result shows that the photoinitiator generated radicals more efficiently per molecule than the

monomer (PEGda). However, cytotoxicity would also increase when the photoinitiator concentration is increased.

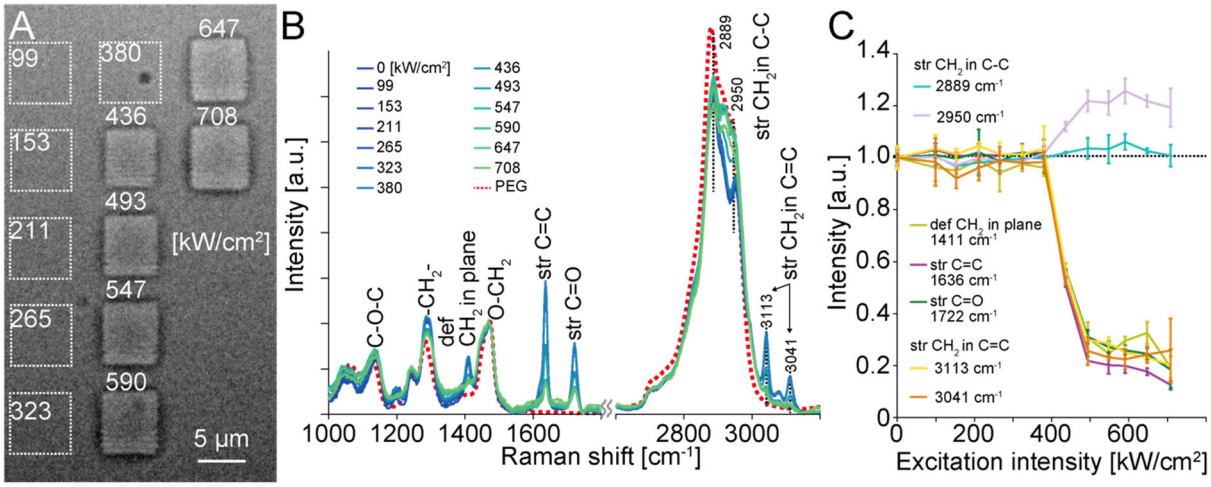

Figure 2. Raman analysis of PEGda upon DUV-TPP. (A) Optical bright-field image of micro-structures which were fabricated with different excitation intensities. (B) Raman spectra of PEGda micro-structures (solid lines) and PEG (dotted line) (C) Plots of Raman peak intensities as a function of excitation intensity for DUV-TPP.

To verify that the properties of the fabricated PEG microstructures were preserved, we investigated their water response. The PEG molecular structures can swell by absorbing water. It has been reported that microstructures fabricated with TPP still exhibit a swelling function in water[15,31]. Water-swollen polymer networks in hydrogels can mimic the mechanical stiffness of the ECM in soft tissue and are helpful for cell attachment[32]. We cast a droplet of 100 µL distilled water on the micro bolt-shaped structures with a thick cylinder on a thin cylinder (**Figure 3**A) which were fabricated using DUV-TPP with excitation intensities from 513 kW/cm^2 to 718 kW/cm^2. (Figure 3B). Figure 3C shows that all the obtained microstructures showed expansion by swelling. We measured the swelling ratio based on the surface area at the top surface of the bolt heads before and after the addition of water. As shown in Figure 3D, the swelling ratio decreases as a function of excitation intensity. This decrease can be related to the cross-linking density at the micro-structure; the higher the excitation intensity for photopolymerization of PEGda, the higher cross-linking

density with less polymer mesh size and, consequently the smaller water swelling[31]. The result indicates that DUV-TPP can be used to fabricate the microstructure of a PEG hydrogel with a water-swollen polymer network.

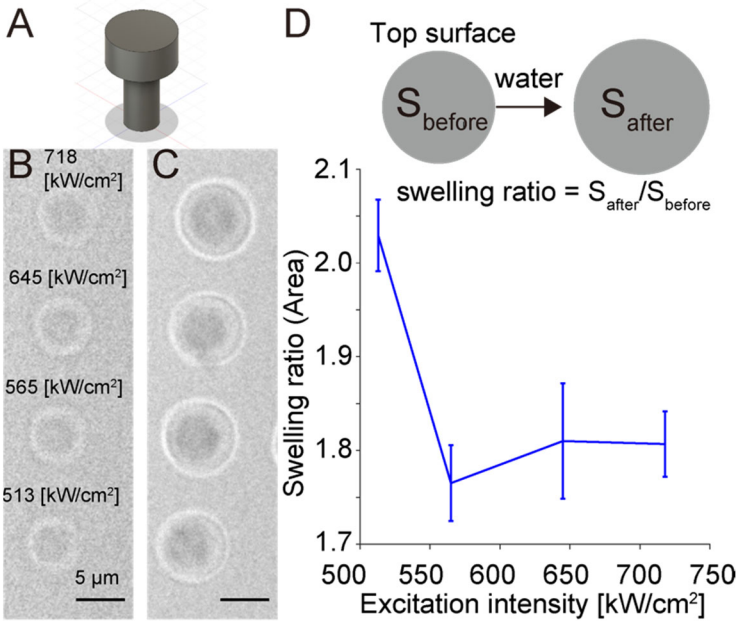

Figure 3. Water response of PEG structures fabricated by DUV-TPP. (A) Design of a micro-structure for measurement (B) Bright-field image of microstructures fabricated from pure PEGda with the excitation intensities from 513 kW/cm^2 to 718kW/cm^2. (C) Bright-field image of the micro-structures after the addition of 100 µL distilled water. Scale bars is 5 µm. (D) A plot of swelling ratio as a function of excitation intensity.

2.2. DUV-TPP of type-I collagen

We performed photoinitiator-free DUV-TPP using type-I collagen, which is one of the ECM proteins. The ECM regulates various cellular functions, such as cell behavior [33], cytoskeleton formation[34], and intercellular communication[35]. Type I collagen is fibrillar collagen present in most organs and is a major component of the ECM. It is particularly abundant in the bones, tendons, and dermis. Type I collagen has been used as a material for 3D fabrication using cross-linking after two-photon absorption by photoinitiators [36–40]. However, the fact that type I collagen is soluble only in acidic aqueous solutions could place a difficulty in the use of

photoinitiators because photoinitiators typically lose their function under acidic conditions [36,38].

Type I collagen absorbs DUV light, especially at 200- 220 nm (Figure S6), by amino acids such as glycine, proline, alanine, and aromatic amino acids, which are major components of collagen. Here, we performed photoinitiator-free fabrication of type I collagen by DUV-TPP. An acidic type I collagen aqueous solution without photoinitiators was prepared and dropped on a coverslip at room temperature. The collagen sample was excited using a visible femtosecond pulsed laser beam (Experimental Section). The focal spot was steered over a cubic region of 5 μm per side. Cubic structures were fabricated at the excitation intensity of 141 kW/cm^2 and higher up to 213 kW/cm^2. **Figure 4**A shows a bright-field image of the structures fabricated with different excitation intensities. The excitation intensity of 141 kW/cm^2 was approximately one-seventieth of the value obtained by direct multiphoton excitation of collagen using a near-infrared femtosecond pulsed laser[41]. Adjusting the two-photon excitation wavelength to match approximate double of the one-photon absorption peak wavelength leads to a more efficient cross-linking reaction.

Figure 4B shows the Raman spectra of the fabricated structures shown in Figure 4A. The solid lines represent the Raman spectra, and the dotted line indicates the baseline calculated using polynomial fitting[42]. The increased baseline with an excitation intensity above 141 kW/cm^2 indicates an increase in autofluorescence from collagen microstructures. Figure 4C shows the Raman spectra after baseline subtraction. According to literature showing intact type I collagen Raman spectra[43–46], The peaks observed in the obtained spectra are interpreted as follows; the peaks at 816 cm^{-1}, 855 cm^{-1}, and 878 cm^{-1} can be assigned to the stretching vibration of C-C, mainly from proline and hydroxyproline; 1003 cm^{-1}, the stretching vibration of C-C bonds in phenylalanine; 1236 cm^{-1}, the amide III band in the random coil structure; 1270 cm^{-1}, the amide III band in the alpha-helix secondary structure; 1451 cm^{-1}, the deformation vibration of CH_3 and CH_2; 1601 cm^{-1}, the ring vibration

in tyrosine and phenylalanine; and 1667 cm^{-1}, the stretching vibration of C=O in the amide I band. Even after two-photon excitation using a visible laser, several Raman peaks at 878 cm^{-1} and 1003 cm^{-1} remained unchanged. Above the intensity of 141 kW/cm^2, two Raman peaks appeared at 1601 cm^{-1} and 1772 cm^{-1}. These two Raman bands correspond to the photoproduct band[47] and the stretching vibration of C=O in COOH, but not in the amide I band, respectively.

Next, we analyzed the intensity of autofluorescence. Figure 4D shows the plot of the baseline intensity obtained with the sum of the baselines between 800 cm^{-1} and 1800 cm^{-1}. The fluorescence baseline intensity increased drastically above the two-photon excitation intensity of 141 kW/cm^2. It has been reported that collagen shows an increase in fluorescence after UV irradiation due to cross-linking[48,49]. It has been experimentally demonstrated that photo-induced cross-linking and fluorescence are derived from aromatic acids [50,51]. It has also been reported that fluorescence from collagen increases after the addition of a photosensitizer and two-photon excitation using a NIR femtosecond laser [52]. In literature, the growth of the fluorescence signal was attributed to formation of di-tyrosine, which was generated by photo-oxidation of the tyrosine side chain [52]. In our study, the increase in fluorescence was probably caused by cross-linking of collagen molecules which was directly induced with a visible femtosecond pulsed laser. On the other hand, we observed that the microstructures with too much excitation intensity for fabrication caused less autofluorescence (Figure S7). It can be explained by the optical breakdown of collagen.

Figure 4E shows a plot of the relative Raman intensity, which was calculated using the ratio of the intensities at 1236 cm^{-1} of amide III mode in the random coil, to those at 1270 cm^{-1} of amide III in the alpha-helix. These Raman bands have been used to identify the secondary structure of collagen[53]. We observed a decrease in the Raman intensity ratio and a large slope of the decrease at 165 kW/cm^2 as the excitation intensity increased. The decrease in the

intensity ratio shows that the secondary structure changed from an alpha helix to a random coil. This structural change has been experimentally reported for DUV irradiation [54].

Figure 4F shows a plot of the Raman peak intensity at 1601 cm^{-1}, normalized by that at 1454 cm^{-1}. The plot also shows a gradual increase below 141 kW/cm^2 and a sharp increase above that. This Raman peak was originally assigned to ring vibrations of tyrosine and phenylalanine. The growth in the Raman band could be attributed to photoproducts generated in collagen from photo-oxidation of amino acid residues, especially tyrosine, histidine, phenylalanine, and methionine, as indicated by photo-oxidation of those amino acids using DUV irradiation[55]. It has also been reported that the Raman bands of these photoproducts were observed around 1600 cm^{-1} in the Raman spectra of proteins and cells after DUV exposure [47]. Moreover, oxidized tyrosine shows a similar Raman band [56]. We experimentally verified that tyrosine solution after DUV-TPP also has Raman spectrum similar to the reported oxidized tyrosine one (Figure S8), indicating that visible-wavelength two-photon excitation onto collagen induced photo-oxidation of tyrosine residues.

Figure 4G shows the plot of the Raman peak intensity at 1772 cm^{-1}. The plot shows a drastic increase above a threshold intensity of 141 kW/cm^2. It has been reported that the appearance of the C=O peak at approximately 1780 cm^{-1} is due to the partial hydrolysis of peptide links within collagen[57]. It is also known that UV exposure to collagen induces the cleavage of its peptide bonds[58–60]. These facts indicate that the cleavage of peptide bonds in collagen was induced in DUV-TPP.

Raman intensities and auto-fluorescence intensity also in Figure 4D-G have nonlinear behavior with a respect to excitation intensity. On the other hand, the irradiation of 400 nm CW light did not show photopolymerization effects even at a 5 times higher excitation intensity (Figure S1), which confirms that the photopolymerization under the visible pulse irradiation did not occur with the linear process. The above results indicate that the oxidation of amino acids and cleavage of peptide bonds in collagen were induced in two-photon

process. In our assumption, the oxidation of aromatic amino acids induces crosslinking of collagen and the cleavage of peptide bonds results in discontinuous collagen structures. These chemical changes led to conformational changes in the random-coiled structure.

We performed further analysis of collagen using liquid chromatography (LC) and mass spectrometry (MS). Dozens of collagen microstructures (800 μm × 800 μm × 5 μm) were prepared with DUV-TPP, were digested with collagenase solution. The detailed pretreatment for LC and MS measurement is described in the experimental section. Figure 4H is fluorescence chromatograms of collagenase digest of collagen with and without DUV-TPP. Excitation and detected emission wavelength were set to 320 nm and 400 nm, respectively. Fluorescence chromatogram of collagen with DUV-TPP shows several distinct peaks at the retention time between 2.5 and 10 min, which are not seen in that without DUV-TPP. Enzymatic degraded peptide fragments with DUV-TPP emit autofluorescence. Figure 4I shows MS spectrum of the eluate with DUV-TPP at 2.8 min retention time, at which collagen with DUV-TPP showed the strongest peak in fluorescence chromatogram. MS spectrum has two characteristic peaks at 861.06, and 877.03 *m/z*, which are not observed in MS spectrum without DUV-TPP, suggesting the mass of fluorescence peptides. According to the LC and MS analysis, visible two-photon excitation generated fluorescent peptides in collagen as a photoproduct.

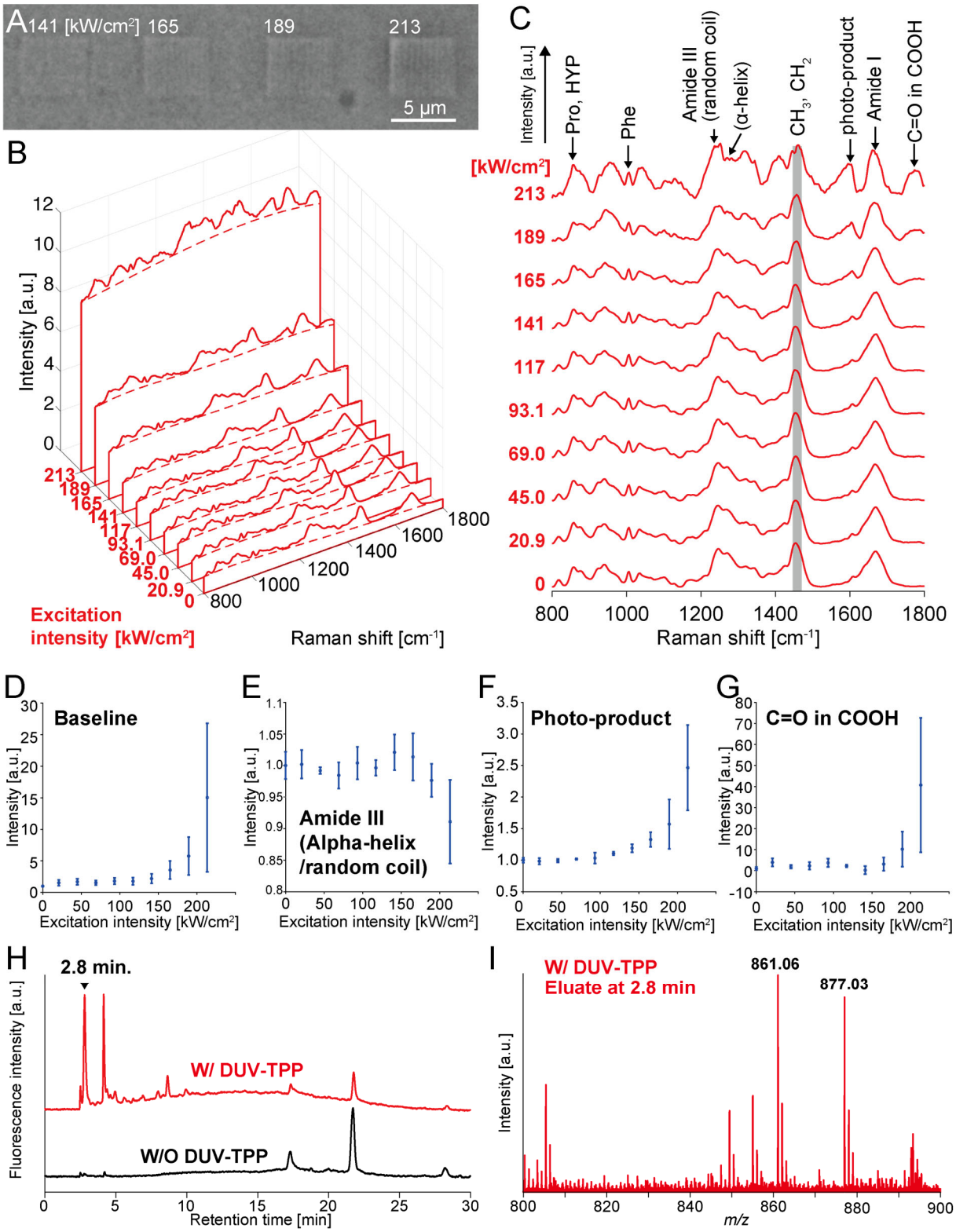

Figure 4. Raman, LC and MS investigation of collagen upon DUV-TPP. (A) Optical bright-field images of microcubes fabricated with different excitation intensities of DUV-TPP. (B) Raman spectra of collagen irradiated with different excitation intensities of DUV-TPP. Solid lines are normalized one. Dotted lines are the baselines. (C) Baseline-subtracted Raman spectra of (B). (D)-(G) Raman peaks plots as a function of excitation intensity of DUV-TPP. (H) Fluorescence chromatograms of digested collagen with (red) and without (black) DUV-

TPP. Excitation and emission wavelength were set to 320 nm and 400 nm, respectively. (I) MS spectrum of HPLC fractioned collagen at the retention time at 2.8 min.

We also examined the enzymatic reaction of collagen after DUV-TPP treatment using collagenase, which specifically fragments peptides in the collagen triple helix. To do this, we fabricated cubic structures with sides of 5 μm using different excitation intensities for DUV-TPP from 191 kW/cm^2 to 450 kW/cm^2. A droplet of collagenase solution in PBS at 37 °C was added to the microstructures. **Figure 5**A shows time-lapse bright-field images of the fabricated microstructures after the addition of collagenase solution. We observed the decay of the image contrast of the microcubes over time with the structures fabricated with laser intensities lower than 450 kW/cm^2. The micro-cube fabricated with an excitation of 450 kW/cm^2 was observed 800 s after the addition of the enzyme. Figure 5B shows plots of the relative darkness, which was calculated by subtracting the value of micro-cubes from that around the micro-cubes as a background. Single exponential fitting of these plots showed that the time for contrast decay increased as the excitation intensity for DUV-TPP increased. The contrast decay of the structure fabricated at 450 kW/cm^2 was two orders of magnitude slower than the others, indicating that triple-helix structures in collagen were mostly destroyed by its high excitation intensity. These results indicate that at an excitation intensity of less than 450 kW/cm^2, DUV-TPP of collagen can be performed with a small degradation in the peptide structure of collagen. Moreover, we performed fluorescence staining with the collagen-binding reagent Col-F, which is also specific to the triple-helix structure. We confirmed that the microstructure of collagen was stained with Col-F, and the microstructure showing the breakdown effect was not stained (Figure S9). Additionally, we confirmed that the fabricated collagen microstructures swelled about 1.7 times in DMEM medium at 37 °C temperature (Figure S10). This indicates that the fabricated collagen microstructures have hydrogel

characteristic. These results conclude that careful tuning of the DUV-TPP conditions can realize the 3D fabrication of collagen while maintaining its intrinsic properties.

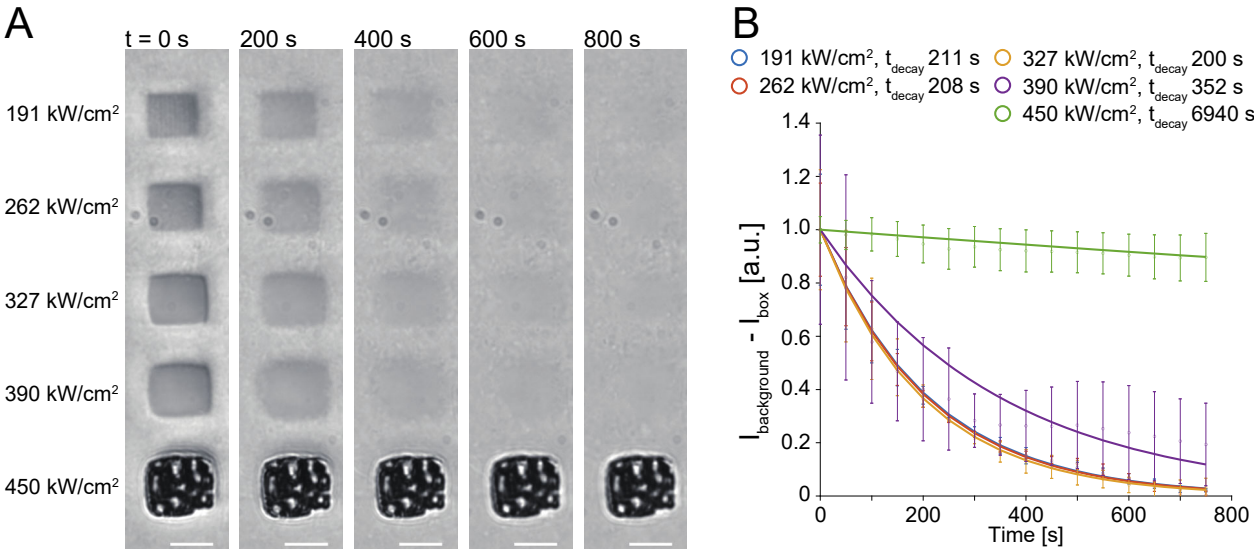

Figure 5. Enzymatic reaction of collagen structures fabricated by DUV-TPP. (A) Time-lapse bright-field images during enzymatic reaction with collagenase. (B) Plots of contrast change and the decay time (t_{decay}) of the collagen microstructure.

We observed 3D micro or nanostructures of collagen by detecting the auto-fluorescence of collagen after irradiation with visible wavelength pulses at 400 nm. Confocal microscopy was used for three-dimensional (3D) imaging. We fabricated a 3D collagen micro-network structure with seven posts connected in lines. We conducted 3D imaging of collagen microstructures without any developmental process because the 3D collagen structures collapsed due to its insufficient stiffness when they were extracted in the air. Fluorescence was collected at 500-550 nm using a 488 nm excitation wavelength. **Figure 6**A shows the obtained 3D optical sectioning images. The lines were only observed at a height of 3 μm. Figure 6B shows the 3D fluorescence image of the fabricated structure. Figure 6C shows a cross-sectional (xz) fluorescence image obtained from the dotted line in Figure 6A. The line structure is free-standing in three dimensions and imaged as a line with FWHM values of 0.340 and 0.610 μm in the lateral and axial directions, respectively. The lateral linewidth was three times smaller than that in a demonstration using NIR femtosecond

pulses[41]. Because the extraction of the 3D structures in the air was not successful, scanning electron images were not obtained in this experiment.

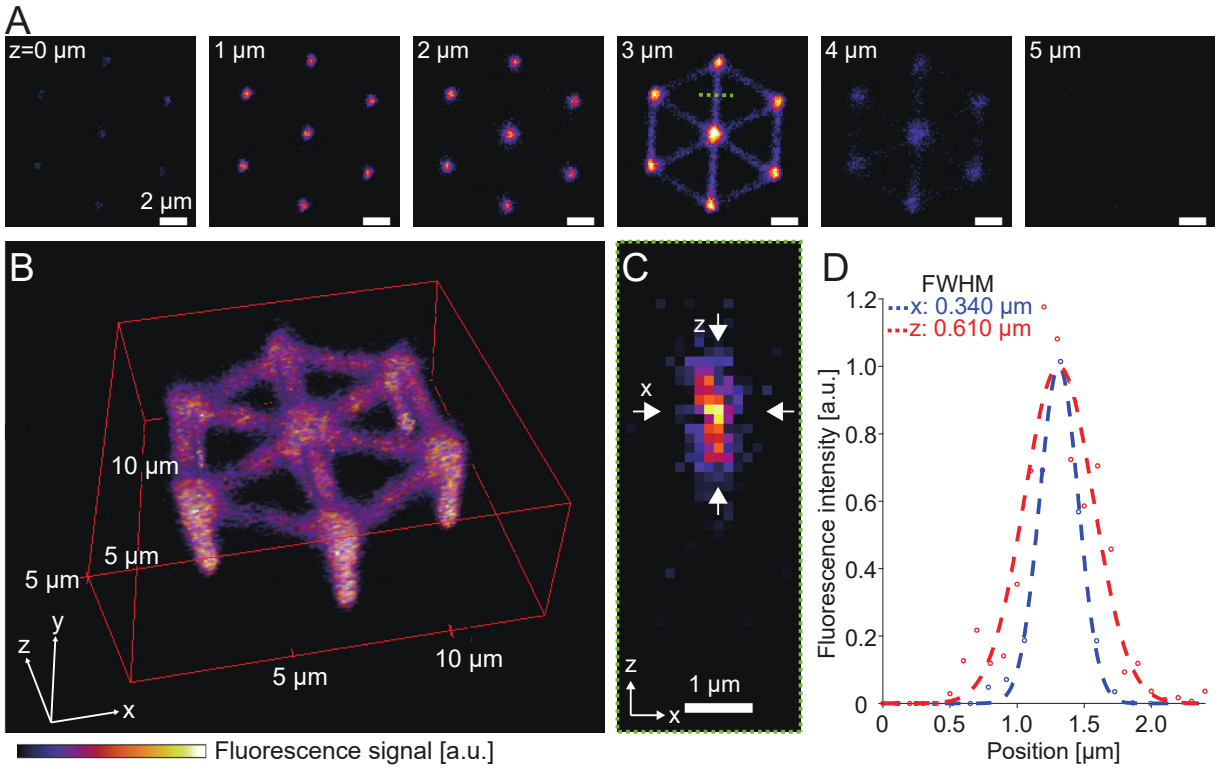

Figure 6. 3D observation of a fabricated collagen micro-structure. (A) 3D optical sectioning with a confocal autofluorescence image of the 3D collagen microstructure. The excitation and detection wavelengths were 488 nm, and 500-550 nm, respectively. The excitation intensity of DUV-TPP was 360 kW/cm2. (B) Reconstructed autofluorescence image of the 3D collagen structure. (C) Cross-sectional (xz) fluorescence image obtained at the dotted line in (A). (D) Line profiles of the micro-structure indicated by arrows in (C) in lateral and axial directions.

3. Conclusion

In this work, we applied photoinitiator-free two-photon polymerization to fabricate micro/nano-scale 3D structures using biocompatible materials PEGda and collagen. We successfully performed 3D microfabrication of these materials with a feature size on the nanometer scale and a higher polymerization efficiency than those obtained using photoinitiators by a longer excitation wavelength. As a future work, it is necessary to increase the stiffness of the 3D collagen structure in order to extract it in the air for biological applications. It can probably be a solution to mix glucose as a cross-linker and conduct photo-

crosslinking of the mixed one[61], or to use collagen chemically modified by (meth)acryloyl groups[62,63].

We elucidated the chemical mechanism of the photoinitiator-free TPP of PEGda and collagen by introducing a Raman spectroscopic system into DUV-TPP. In PEGda, the C=C bonds are consumed for two-photon polymerization, even without photoinitiators. In collagen, we found that cross-linking via photooxidation of aromatic amino acids and cleavage of peptide bonds occurred simultaneously, leading to a partial change in the secondary structures of collagen. We confirmed that the water swelling of the PEGda microstructures was similar to that of the fabrication using a NIR femtosecond pulsed laser and a photo-initiator. We also observed that the microstructures of collagen without optical breakdown can maintain the enzymatic properties of collagenase. These results indicate that the material-specific characteristics of each material are preserved even after DUV-TPP.

DUV-TPP can be a method for fabrication of a 3D cell culturing scaffold with a single cell scale. Since DUV-TPP does not use photoinitiator, the fabricated structures probably have more biocompatible than that fabricated with TPP using photoinitiators. By creating 3D microstructures with DUV-TPP and seeding cells on the microstructures, cells can be cultured in a 3D environment with less cytotoxicity. On the other hand, DUV-TPP may not be used for the 3D fabrication in the presence of living cells because cells can also be excited via one- or two-photon absorption. When considering the encapsulation of cells, using NIR wavelength for excitation is more appropriate due to the less cell damage during light irradiation[15,64,65].

In principle, DUV-TPP is highly feasible for application to other biocompatible materials with absorption in the deep-UV region, such as functionalized biodegradable polymers or other ECM proteins. DUV-TPP can expand the range of materials used to fabricate 3D cell scaffolds with high biocompatibility. Using a shorter wavelength would expand the range of chemical bonds available for DUV-TPP, possibly providing more efficient excitation with a better spatial resolution. The challenge of low-throughput

fabrication in two-photon polymerization remains but as DUV-TPP requires a lower excitation intensity than that of TPP using NIR light does, it has the potential of higher throughput by combining existing technologies, such as multi-focus excitation[66] or 2D projection based on spatiotemporal focusing[67], which have been developed for NIR-TPP.

4. Experimental section

Optical system for DUV-TPP fabrication and in-situ Raman spectroscopy

Figure 7 shows an optical system for performing DUV-TPP fabrication and the Raman spectra of materials *in situ* before and after DUV-TPP. The light source for two-photon excitation was a mode-locked Ti: sapphire laser (Tsunami, Spectra Physics) oscillating at a center wavelength of 800 nm with a pulse width of 80 fs and repetition rate of 82 MHz. The 800-nm femtosecond pulses were converted to 400-nm pulses via second harmonic generation by focusing on a BBO crystal (CASTECH INC.) through a lens (L1, f=50 mm, AC254-050-B-ML, Thorlabs). The generated visible pulsed laser was collimated by another lens (L2, f=100 mm, AC254-100-A-ML, Thorlabs), expanded by a couple of lenses (L3, f=30 mm, AC254-30-A-ML, Thorlabs; L4, f=150 mm, AC254-150-A-ML), and extracted through a bandpass filter with a center wavelength of 400 nm (FBH400-40, Thorlabs). The visible femtosecond pulses were reflected on two dichroic mirrors (DM1, DMLP505, Thorlabs; DM2, FF665-Di02-25×36, Semrock) and focused onto a sample with an oil-immersion objective (NA1.45, UPlanApo, OLYMPUS). The sample was set on a 3-axes piezoelectric stage (P-517, Physik Instrumente) and steered in three dimensions relative to the fixed focal spot.

We used a 532-nm solid-state CW laser (Samba, Cobolt) as the light source for Raman excitation. The excitation laser beam was collimated and expanded with a couplel of lenses (L3, f=30 mm, AC254-030-A-ML; L4, f=200 mm, AC254-200-A-ML). The expanded beam was reflected at two dichroic mirrors (DM2, FF665-Di02-25×36, Semrock; DM3, Di02-

R532-25×36, Semrock) and focused with the same objective lens onto the sample. Scattering from the samples was collected through the objective. Raman scattering data were extracted using DM1 and a long-pass filter (LP, LP02-532RU-25). Raman spectra were obtained using a spectrophotometer (SP300i, Princeton Instrument Acton) equipped with a cooled charge-coupled device (CCD) camera (Spec10: 400BR, Princeton Instruments) through a lens (L7 f=200 mm, AC254-200-A-ML). We used a grating with a blaze wavelength of 500 nm and 600 grooves/mm for Raman measurements.

Sample preparation

PEGda (700 Mn) from Sigma was used without any purification. For the fabrication of hydrogel PEGda, a 20 μL droplet of pure PEGda was cast on a MAS-coated coverslip (MAS-GP, Matsunami). When measuring a UV-Visible absorption spectrum of PEGda, we diluted PEGda in water to a concentration of 2 wt%.

A solution of collagen type I (3 mg) under acidic conditions was purchased from Nitta Gelatin (Cellmatrix type I-A). Collagen solution (60 μL) was dropped on a coverslip (MAS-GP, Matsunami) and dried at room temperature for 30 min, which increased the concentration of collagen molecules.

Fabrications

The fabricated structures were designed using 3D CAD software. The trajectory of the focal spot during TPP fabrication was calculated based on the G-code. The exposure time for fabrication was 4 ms/voxel for all experiments. The light intensity for TPP was changed from 0 kW/cm^2 to approximately 700 kW/cm^2 depending on the purpose of the experiments. For the Raman spectroscopy study, we fabricated a cubic structure with a side of 5 μm. The light intensity at a sample plane was calculated by dividing the average power by the spot size, $\pi (0.61 \lambda /\mathrm{NA})^2$.

Raman measurements and analysis

For Raman measurements of the PEGda samples, the exposure time of the CCD camera and the Raman excitation intensity was 10 s and 2700 kW/cm^2, respectively. The width of the slits was 40 μm.

When we used collagen as a sample, we set the CCD camera exposure time at 60 s, slit width at 40 μm, and excitation intensity at 2700 kW/cm^2. We applied Savitzky-Golay filtering with a polynomial order of 3 and frame length of 5 to the obtained Raman spectra. Baseline correction using a modified polyfit fluorescence removal method[42] was applied to the Raman spectra to plot the Raman intensities of several Raman peaks as a function of the excitation intensity for DUV-TPP.

Scanning electron microscope observation of PEG micro-structures

To observe the microstructure of PEGda, the fabricated microstructure was extracted using ethanol and covered with a platinum layer of 2 nm thickness. The microstructure was observed using a field-emission scanning electron microscope (S4800, Hitachi).

Liquid chromatograph (LC) and mass spectrometry (MS) of collagen

Fabricated collagen structures on a coverslip were collected in a tube by scratching surface of the coverslip with tweezers, incubated in 37 °C collagenase solution for digestion in 30 min, and freeze-dried. The freeze-dried sample was dissolved in 50 μL water-acetonitrile mixture (95/5; v/v) containing 0.1% trifluoroacetic acid, and filtered with 0.45 μm pore sizes (Millex-LH, Merck-Millipore). 10 μL solution was injected into a high-performance liquid chromatography (HPLC) system composing of an Inertsil ODS-3 column (4.6 × 250 mm; GL Sciences, Inc.), a pump (PU-2087, JASCO Corporation), and a fluorescence detector (FP-2020, JASCO Corporation) at a flow rate at 1 mL/min. We set excitation wavelength and detected fluorescence wavelength to 320 nm and 400 nm, respectively. We used mobile-phase A (0.1% TFA in distilled water) and mobile-phase B (0.1% TFA in acetonitrile) to make a gradient condition as 5-50% B in 30 min. The fractionated eluate was freeze-dried, and dissolved in 10 mg/mL α-cyano-4-hydroxycinnamic acid in water-acetonitrile mixture (10/90;

v/v) containing 0.1% trifluoroacetic acid. The eluate solution was deposited on a MALDI plate. MS spectrum was acquired with a MALDI-TOF MS system in positive ion mode (JMS-S3000 SpiralTOF^{TM}-plus2.0, JEOL Ltd.).

Enzymatic degradation of collagen

Collagenase (FUJIFILM Wako Pure Chemical Corporation) was dissolved in PBS at a concentration of 0.8 mg/mL. The collagen solution warmed to 37 °C was dropped onto collagen microcubes with a side of 5 μm. We observed the enzymatic degradation of the microcubes with time-lapse optical bright-field imaging using the same objective lens as used for DUV-TPP fabrication. We plotted the changes in image contrast by enzymatic degradation, calculated by subtracting the light intensity on the microcubes from that around the microcubes. The decay time of the enzymatic degradation was estimated by fitting an exponential function.

Confocal fluorescence imaging of collagen micro-structures

We used a confocal fluorescence microscope (A1, Nikon) for the 3D observation of collagen microstructures. The excitation wavelength was 488 nm. An objective lens (60×, NA1.4, oil immersion, Plan Apo VC60×Oil DIC N2 Nikon) was used. The wavelength range for fluorescence detection was 500–550 nm. The diameter of the pinhole was tuned to be 0.5 Airy units (AU).

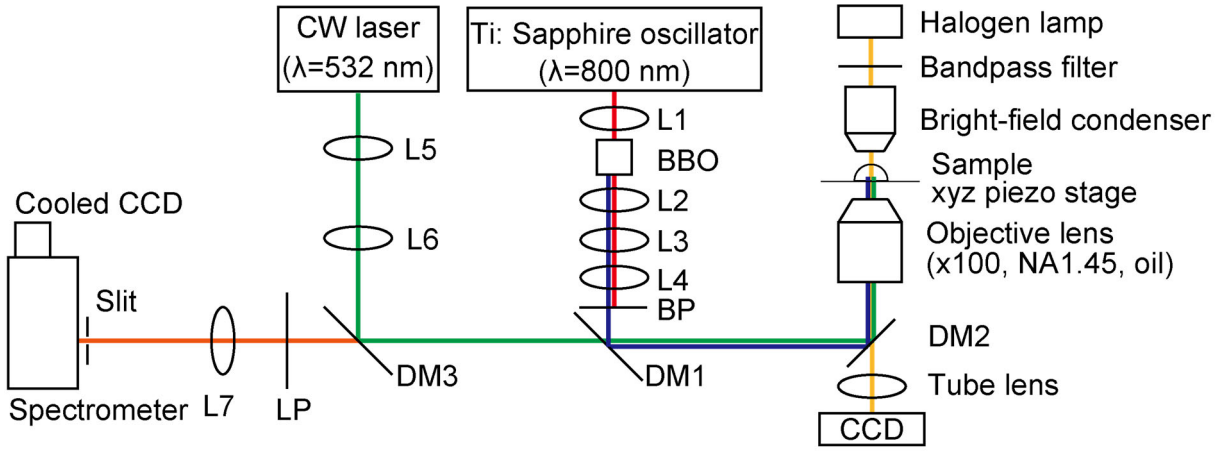

Figure 7. Experimental setup for two-photon polymerization (TPP) fabrication and *in-situ* Raman spectroscopic measurement. L: lens, BP: bandpass filter, FM: flip mount mirror, DM: dichroic mirror, LP: long-pass filter.

Supporting Information

The following files are available free of charge.

CW laser irradiation of PEGda and collagen, The achievement of 30-nm linewidth by using 4arm-PEG acrylate, the overdose of the excitation to PEGda, Raman analysis of 4arm-PEG acrylate upon DUV-TPP, Excitation intensity threshold of PEGda with phototinitiator in TPP, UV-visible absorption spectrum of collagen, auto-fluorescence of collagen microstructures fabricated with DUV-TPP, DUV-TPP of tyrosine, and staining of collagen microstructures with collagen binding probe.

Conflict of interest

The authors declare the following competing financial interest(s): A.T. and K.F. are joint inventors of a patent application of the photolithography technique described in the paper

Acknowledgments

This work was supported in part by JSPS KAKENHI Grant Number JP 20K21130, JST COI-NEXT under Grant Number JPMJPF2009, and JST SPRING Grant Number JPMJSP2138.

The authors thank Prof. Michiya Matsusaki of Osaka University for his helpful advice on the enzymatic degradation and immunostaining of collagen.

Received: ((will be filled in by the editorial staff))

Revised: ((will be filled in by the editorial staff))

Published online: ((will be filled in by the editorial staff))

References

[1] S. Maruo, O. Nakamura, S. Kawata, *Opt. Lett.* **1997**, *22*, 132.

[2] S. Kawata, H.-B. Sun, T. Tanaka, K. Takada, *Nature* **2001**, *412*, 697.

[3] A. Ovsianikov, M. Malinauskas, S. Schlie, B. Chichkov, S. Gittard, R. Narayan, M. Löbler, K. Sternberg, K. P. Schmitz, A. Haverich, *Acta Biomater.* **2011**, *7*, 967.

[4] B. Kaehr, R. Allen, D. J. Javier, J. Currie, J. B. Shear, *Proc. Natl. Acad. Sci. U. S. A.* **2004**, *101*, 16104.

[5] J. C. Harper, S. M. Brozik, C. J. Brinker, B. Kaehr, *Anal. Chem.* **2012**, *84*, 8985.

[6] V. Melissinaki, A. A. Gill, I. Ortega, M. Vamvakaki, A. Ranella, J. W. Haycock, C. Fotakis, M. Farsari, F. Claeyssens, *Biofabrication* **2011**, *3*, 045005.

[7] D. Kuznetsova, A. Ageykin, A. Koroleva, A. Deiwick, A. Shpichka, A. Solovieva, S. Kostjuk, A. Meleshina, S. Rodimova, A. Akovanceva, D. Butnaru, A. Frolova, E. Zagaynova, B. Chichkov, V. Bagratashvili, P. Timashev, *Biofabrication* **2017**, *9*, 025009.

[8] M. Iosin, T. Scheul, C. Nizak, O. Stephan, S. Astilean, P. Baldeck, *Microfluid. Nanofluidics* **2011**, *10*, 685.

[9] S. Hengsbach, A. D. Lantada, *Biomed. Microdevices* **2014**, *16*, 617.

[10] R. Bail, A. Patel, H. Yang, C. M. Rogers, F. R. A. J. Rose, J. I. Segal, S. M. Ratchev, *Procedia CIRP* **2013**, *5*, 222.

[11] C. G. Williams, A. N. Malik, T. K. Kim, P. N. Manson, J. H. Elisseeff, *Biomaterials* **2005**, *26*, 1211.

[12] D. Serien, K. Sugioka, *ACS Biomatr. Sci. Eng.* **2020**, *6*, 1279.

[13] A. Taguchi, A. Nakayama, R. Oketani, S. Kawata, K. Fujita, *ACS Appl. Nano Mater.* **2020**, *3*, 11434.

[14] J. E. Koskela, S. Turunen, L. Ylä-Outinen, S. Narkilahti, M. Kellomäki, *Polym. Adv. Technol.* **2012**, *23*, 992.

[15] J. Torgersen, A. O. V. Mironov, N. Pucher, X. Qin, Z. Li, K. Cicha, T. Machacek, R. Liska, V. Jantsch, J. Stampfl, *J. Biomed. Opt.* **2012**, *17*, 15.

[16] S. H. Lee, J. J. Moon, J. L. West, *Biomaterials* **2008**, *29*, 2962.

[17] Y. C. Zheng, Y. Y. Zhao, M. L. Zheng, S. L. Chen, J. Liu, F. Jin, X. Z. Dong, Z. S. Zhao, X. M. Duan, *ACS Appl. Mater. Interfaces* **2019**, *11*, 1782.

[18] K. Takada, D. Wu, Q.-D. Chen, S. Shoji, H. Xia, S. Kawata, H.-B. Sun, *Opt. Lett.* **2009**, *34*, 566.

[19] Y. Bougdid, I. Maouli, A. Rahmouni, K. Mochizuki, I. Bennani, M. Halim, Z. Sekkat, *J. Micromechanics Microengineering* **2019**, *29*, DOI: 10.1088/1361-6439/aafda0.

[20] E. Gontran, M. Juchaux, C. Deroulers, S. Kruglik, N. Huang, M. Badoual, O. Seksek, *J. Appl. Polym. Sci.* **2018**, *135*, 1.

[21] H. G. M. Edwards, K. S. Johal, A. F. Johnson, *Vib. Spectrosc.* **2006**, *41*, 160.

[22] S. Damoun, R. Papin, G. Ripault, M. Rousseau, J. C. Rabadeux, D. Durand, *J. Raman Spectrosc.* **1992**, *23*, 385.

[23] P. Hayden, H. Melville, *J. Polym. Sci.* **1960**, *43*, 215.

[24] H. Li, Y. Cheng, H. Tang, Y. Bi, Y. Chen, G. Yang, S. Guo, S. Tian, J. Liao, X. Lv, S. Zeng, M. Zhu, C. Xu, J. X. Cheng, P. Wang, *Adv. Sci.* **2020**, *7*, 1903644.

[25] S. Mishra, F. J. Scarano, P. Calvert, *J. Biomed. Mater. Res. - Part A* **2012**, *100 A*, 2829.

[26] K. Cicha, Z. Li, K. Stadlmann, A. Ovsianikov, R. Markut-Kohl, R. Liska, J. Stampfl, *J. Appl. Phys.* **2011**, *110*, 064911.

[27] L. J. Jiang, Y. S. Zhou, W. Xiong, Y. Gao, X. Huang, L. Jiang, T. Baldacchini, J. Silvain, Y. F. Lu, *Opt. Lett.* **2014**, *39*, 3034.

[28] T. Scherzer, W. Knolle, S. Nanmov, L. Prager, *Macromol. Symp.* **2005**, *230*, 173.

[29] H. Yu, H. Ding, Q. Zhang, Z. Gu, M. Gu, *Light Adv. Manuf.* **2021**, *2*, 1.

[30] W. Gao, H. Chao, Y.-C. Zheng, W.-C. Zhang, J. Liu, F. Jin, X.-Z. Dong, Y.-H. Liu, S.-J. Li, M.-L. Zheng, *ACS Appl. Mater. Interfaces* **2021**, DOI: 10.1021/acsami.1c02227.

[31] C. Lv, X. C. Sun, H. Xia, Y. H. Yu, G. Wang, X. W. Cao, S. X. Li, Y. S. Wang, Q. D. Chen, Y. De Yu, H. B. Sun, *Sensors Actuators, B Chem.* **2018**, *259*, 736.

[32] M. W. Tibbitt, K. S. Anseth, *Biotechnol Bioeng.* **2009**, *103*, 655.

[33] R. Singhvi, A. Kumar, G. P. Lopez, G. N. Stephanopoulos, D. I. C. Wang, G. M. Whitesides, D. E. Ingber, *Science (80-.).* **1994**, *264*, 696.

[34] B. Geiger, A. Bershadsky, R. Pankov, K. M. Yamada, *Nat. Rev. Mol. Cell Biol.* **2001**, *2*, 793.

[35] P. A. Janmey, R. T. Miller, *J. Cell Sci.* **2011**, *124*, 9.

[36] S. Basu, L. P. Cunningham, G. D. Pins, K. A. Bush, R. Taboada, A. R. Howell, J. Wang, P. J. Campagnola, *Biomacromolecules* **2005**, *6*, 1465.

[37] A. Bell, M. Kofron, V. Nistor, *Biofabrication* **2015**, *7*, DOI: 10.1088/1758-5090/7/3/035007.

[38] M. Iosin, O. Stephan, S. Astilean, A. Duperray, M. Iosin, O. Stephan, S. Astilean, A. Duperray, P. B. Microstructura-, *J. Optoelectron. Adv. Mater.* **2007**, *9*, 716.

[39] N. I. Smith, K. Fujita, O. Nakamura, S. Kawata, *Appl. Phys. Lett.* **2001**, *78*, 999.

[40] S. J. J. Kwok, I. A. Kuznetsov, M. Kim, M. Choi, G. Scarcelli, S. H. Yun, *Optica* **2016**, *3*, 469.

[41] M. Gebinoga, J. Katzmann, U. Fernekorn, J. Hampl, F. Weise, M. Klett, A. Läffert, T. A. Klar, A. Schober, *Eng. Life Sci.* **2013**, *13*, 368.

[42] C. A. Lieber, A. Mahadevan-Jansen, *Appl. Spectrosc.* **2003**, *57*, 1363.

[43] B. G. Frushour, J. L. Koenig, *Biopolymers* **1975**, *14*, 379.

[44] W. T. Cheng, M. T. Liu, H. N. Liu, S. Y. Lin, *Microsc. Res. Tech.* **2005**, *68*, 75.

[45] C. J. Frank, R. L. McCreary, D. C. B. Redd, *Anal. Chem.* **1995**, *67*, 777.

[46] I. Notingher, C. Green, C. Dyer, E. Perkins, N. Hopkins, C. Lindsay, L. L. Hench, *J. R. Soc. Interface* **2004**, *1*, 79.

[47] Y. Kumamoto, A. Taguchi, N. I. Smith, S. Kawata, *Biomed. Opt. Express* **2011**, *2*, 927.

[48] E. Fujimori, *Biochemistry* **1966**, *5*, 1034.

[49] M. Wisniewski, A. Sionkowska, H. Kaczmarek, S. Lazare, V. Tokarev, C. Belin, *J. Photochem. Photobiol. A Chem.* **2007**, *188*, 192.

[50] G. Leo, C. Altucci, S. Bourgoin-voillard, A. M. Gravagnuolo, R. Esposito, G. Marino, C. E. Costello, R. Velotta, L. Birolo, *Rapid Commun Mass Spectrom.* **2013**, *27*, 1.

[51] F. Itri, D. M. Monti, B. Della Ventura, R. Vinciguerra, M. Chino, F. Gesuele, A. Lombardi, R. Velotta, C. Altucci, L. Birolo, R. Piccoli, A. Arciello, *Cell. Mol. Life Sci.* **2016**, *73*, 637.

[52] C. Wang, M. Fomovsky, G. Miao, M. Zyablitskaya, S. Vukelic, *Nat. Photonics* **2018**, *12*, 416.

[53] R. J. H. Clark, R. E. Hester, *Spectroscopy of Biological Systems*, John Wiley & Sons, **1986**.

[54] C. A. Miles, A. Sionkowska, S. L. Hulin, T. J. Sims, N. C. Avery, A. J. Bailey, *J. Biol. Chem.* **2000**, *275*, 33014.

[55] D. I. Pattison, A. S. Rahmanto, M. J. Davies, *Photochem. Photobiol. Sci.* **2012**, *11*, 38.

[56] T. M. Cooper, D. L. Bolton, S. T. Schuschereba, E. T. Schmeisser, *Appl. Spectrosc.* **1987**, *41*, 661.

[57] M. Fields, N. Spencer, J. Dudhia, P. F. McMillan, *Biopolymers* **2017**, *107*, 1.

[58] A. Kamińska, A. Sionkowska, *Polym. Degrad. Stab.* **1996**, *51*, 19.

[59] A. Torikai, H. Shibata, *J. Appl. Polym. Sci.* **1999**, *73*, 1259.

[60] A. Sionkowska, *Polym. Degrad. Stab.* **2000**, *68*, 147.

[61] M. P. Ohan, K. S. Weadock, M. G. Dunn, *J Biomed Res* **2002**, *60*, 384.

[62] T. Defize, J. M. Thomassin, H. Ottevaere, C. Malherbe, G. Eppe, R. Jellali, M. Alexandre, C. Jérôme, R. Riva, *Macromolecules* **2019**, *52*, 444.

[63] I. D. Gaudet, D. I. Shreiber, *Biointerphases* **2012**, *7*, 1.

[64] A. Ovsianikov, S. Mühleder, J. Torgersen, Z. Li, X. H. Qin, S. Van Vlierberghe, P. Dubruel, W. Holnthoner, H. Redl, R. Liska, J. Stampfl, *Langmuir* **2014**, *30*, 3787.

[65] M. Tromayer, A. Dobos, P. Gruber, A. Ajami, R. Dedic, A. Ovsianikov, R. Liska, *Polym. Chem.* **2018**, *9*, 3108.

[66] J. I. Kato, N. Takeyasu, Y. Adachi, Sun Hong-Bo, S. Kawata, *Appl. Phys. Lett.* **2005**, *86*, 1.

[67] P. Somers, Z. Liang, J. E. Johnson, B. W. Boudouris, L. Pan, X. Xu, *Light Sci. Appl.* **2021**, *10*, DOI: 10.1038/s41377-021-00645-z.